

## Self-Tuning Yaw Control Strategy of an Horizontal Axis Wind Turbine based on Machine Learning

Aitor Saenz-Aguirre, Ekaitz Zulueta, Unai Fernandez-Gamiz  
Jose Antonio Ramos-Hernanz and Jose Manuel Lopez-Guede

**Abstract** The design procedure of a Machine Learning (ML) based yaw control strategy for an Horizontal Axis Wind Turbine (HAWT) is presented in the following chapter. The proposed yaw control strategy is based on the interaction of three different Artificial Intelligence (AI) techniques to design a ML system: Reinforcement Learning (RL), Artificial Neural Networks (ANN) and metaheuristic optimization algorithms. The objective of the designed control strategy is to achieve, after a training stage, a fully autonomous performance of the wind turbine yaw control system for different input wind scenarios while optimizing the electrical power generated by the wind turbine and the mechanical loads due to the yaw rotation. The RL algorithm is known to be able to learn from experience. The training process could be carried out online with real-time data of the operation of the wind turbine or offline, with simulation data. The use of an ANN to store the data of the matrix  $Q(s,a)$  related to the RL algorithm eliminates the large scale data management and simplifies the operation of the proposed control system. Finally, the implementation of a metaheuristic optimization algorithm, in this case a Particle Swarm Optimization (PSO) algorithm, allows calculation of the optimal yaw control action that responds to the compromise between the generated power increment and the mechanical loads increase due to the yaw actuation.

**Keywords** Wind Turbine Control; Yaw Control; Reinforcement Learning; Artificial Neural Network; Optimization; Pareto Front.

---

A. Saenz-Aguirre (✉) · E. Zulueta · J.M. Lopez-Guede  
Automatic control and System Engineering Dep., University of the Basque Country, Nieves Cano 12,  
01006 Vitoria-Gasteiz, Araba, Spain  
email: asaenz012@ehu.es

E. Zulueta  
email: ekaitz.zulueta@ehu.es

J.M. Lopez-Guede  
email: jm.lopez@ehu.es

U. Fernandez-Gamiz  
Nuclear Engineering and Fluid Mechanics Dep., University of the Basque Country, Nieves Cano 12,  
01006 Vitoria-Gasteiz, Araba, Spain  
email: unai.fernandez@ehu.es

J.A. Ramos-Hernanz  
Electrical Engineering Dep., University of the Basque Country, Nieves Cano 12, 01006 Vitoria-Gasteiz,  
Araba, Spain  
email: josean.ramos@ehu.es

## 55 Abbreviation and Acronyms

56

57	ML	Machine Learning
58	HAWT	Horizontal Axis Wind Turbine
59	AI	Artificial Intelligence
60	RL	Reinforcement Learning
61	ANN	Artificial Neural Network
62	PSO	Particle Swarm Optimization
63	LCOE	Levelized Cost of Energy
64	MLP-BP	MultiLayer Perceptron with BackPropagation
65	MDP	Markov Decision Process
66	DP	Dynamic Programming
67	MC	Monte Carlo
68	TD	Temporal Differences
69	PoF	Pareto optimal Front
70	GA	Genetic Algorithm
71	DE	Differential Evolution
72	PID	Proportional Integral Derivative
73	FAST	Fatigue, Aerodynamics, Structure and Turbulence
74	NREL	National Renewable Energies Laboratory
75	MSE	Mean Squared Error
76	DM	Decision Making

77

78

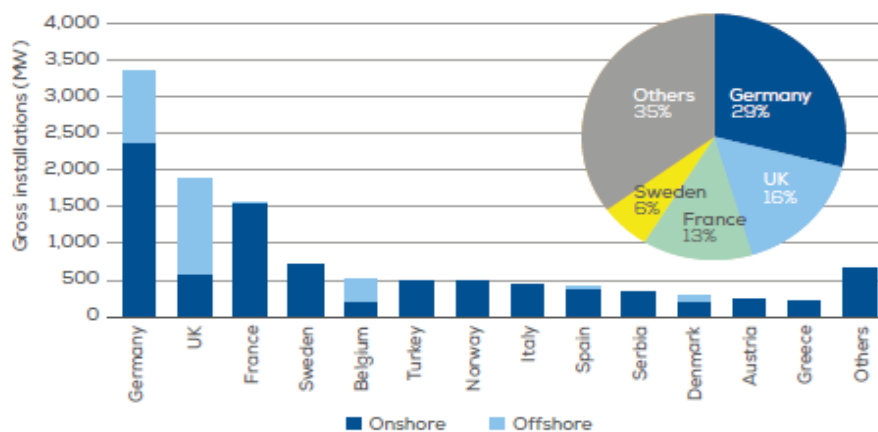
### III-16.1. Introduction

79

80 The gradual depletion of the fossil fuels and the atmospheric pollution originated by their combustion  
81 have brought an important growth of the renewable energy generation systems. Plus, as a result of the yearly  
82 increasing electrical power consumption, the research work with the objective of enhancing the efficiency  
83 of renewable energy systems and maximize their power production has been placed on the focus of many  
84 research institutes and universities [1].

85

86 The most important renewable energy generation source nowadays is the wind energy. Many studies  
87 showing the positive tendency of the wind energy these days can be found in the literature. For example,  
88 according to some studies presented by Rosales-Asensio et al. [2], the sustainable power production with  
89 wind origin in Denmark achieved a 40% of the power produced in the country in 2015. This same value  
90 was quite smaller in Spain, with a 17% in 2015, but having raised from a 10.4% in 2007. More recent  
91 studies elaborated by WindEurope [3], and summarized in Figure III-16.1, show remarkable increments in  
92 the wind energy installed power in 2018 especially in four countries: a 29% in Germany, a 16% in the  
93 United Kingdom, a 13% in France and a 6% in Sweden. All these data indicate the importance of the wind  
94 energy to lead the change of the electrical power generation structures towards a sustainable generation in  
the coming years.



95

96

Figure III-16.1. Wind energy generation increase during year 2018 in some European countries [3]

97 The power generation increase in wind energy systems is tightly related to the investigation work carried  
98 out to reduce the Levelized Cost of Energy (LCOE) of the wind turbines, which encourages capital invest-  
99 ment in the sector. An optimization exercise to reduce the LCOE of a 10 MW wind turbine is presented in  
100 the work of Nyanteh et al. [4]. One main topic of this research work is the development of advanced control  
101 strategies to optimize the performance of the wind turbines. In this context, a robust  $H_{\infty}$  controller to en-  
102 hance the operation and reduce the mechanical loads of a wind turbine is presented by Kim et al. [5]. In the  
103 work of Merabet et al. [6] a Sliding Mode Control strategy is introduced to the control system of a wind  
104 turbine.

105 In this chapter, the design procedure of a yaw control system of an Horizontal Axis Wind Turbine  
106 (HAWT) based on Machine Learning (ML) is presented. The designed intelligent control system is based  
107 on the interrelation of a Reinforcement Learning (RL) algorithm, detailed in the work of Watkins et al. [7],  
108 an Artificial Neural Network (ANN) in form of a MultiLayerPerceptron with BackPropagation (MLP-BP),  
109 presented by Erdogmus et al. [8], and a Particle Swarm Optimization (PSO) metaheuristic algorithm, intro-  
110 duced in the work of Ho et al. [9].

111 The objective of the ML based control strategy developed in this chapter is to achieve a fully autonomous  
112 performance of the yaw system of the wind turbine based on its own experience, which could be acquired  
113 via an offline training, i.e., when the wind turbine is paused, or an online training, i.e., during operation of  
114 the wind turbine. An offline training process is proposed in this chapter. However, a continuous online  
115 training process with real data acquired during operation of the wind turbine to continuously learn from  
116 experience could be implemented as well. The MLP-BP is used to store the data of the matrices  $Q(s,a)$   
117 related to the RL algorithm and manage them as continuous functions,  $Q(s(t),a(t))$ . This process avoids  
118 quantification and large data management problems. The combination of an RL strategy and an ANN is  
119 widely known as Deep Reinforcement Learning [10,11]. An example of the RL and ANN based yaw control  
120 strategy to autonomously maximize the power generated by a wind turbine is presented in the work of  
121 Saenz-Aguirre et al. [12]. Finally, with the introduction of additional features based on the multivariable  
122 PSO optimization algorithm, an increment of the power generated by the wind turbine with a considerable  
123 reduction of the mechanical loads due to the yaw rotation is expected to be achieved.

124 This chapter is structured as follows: the objectives and applications of the proposed yaw control strategy  
125 are presented in Section III-16.2. Section III-16.3 details the theoretical basis of the different Artificial  
126 Intelligence (AI) techniques used to design the ML system. The design procedure of the yaw control system  
127 based on ML is exposed in Section III-16.4. Finally, Section III-16.5 presents the conclusions.

128  
129

### III-16.2. Objectives and Applications

130 The main factor that determines the power output of a wind turbine is the wind incident to its rotor.  
131 However, the wind is originated as a result of very complex meteorological processes, which, as stated by  
132 Bivona et al. [13], are very complex to model, and can, thus, suffer from unpredictable important variations.  
133 Some wind gusts can even exceed the safe wind speed operation range of the wind turbine and endanger  
134 its correct performance. To avoid this issue, a control system is implemented in the wind turbines.

135 The control system of a wind turbine is formed by different control strategies designed to regulate the  
136 rotational speed of the rotor in the whole range of operating points of the wind turbine. A scheme of the  
137 different control loops oriented to regulate the rotational speed of the rotor is presented in Figure III-16.2  
138 (a). As a result of these control strategies, the power output of the wind turbine is predefined for the whole  
139 range of wind speed values in which the turbine operates. The curve that relates the power output of the  
140 wind turbine with the wind speed is known as the power curve. The power curve of the NREL 5MW wind  
141 turbine, presented in the work of Jonkman et al. [14], is illustrated in Figure III-16.2 (b).

142

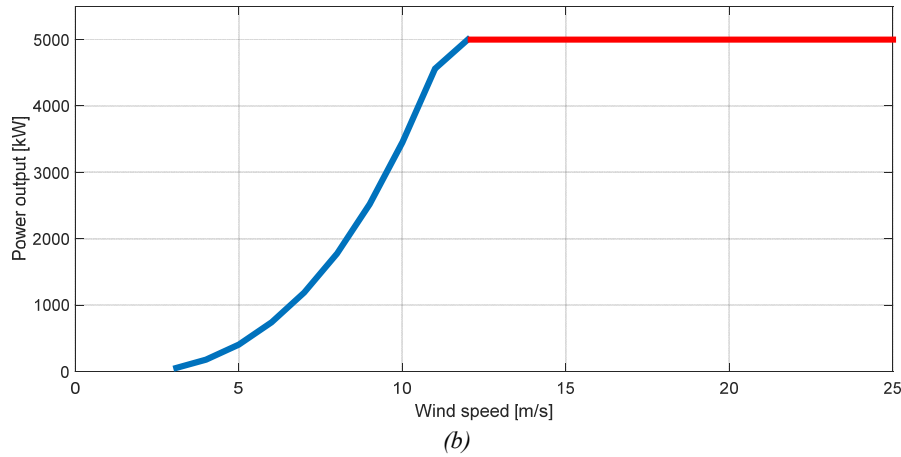
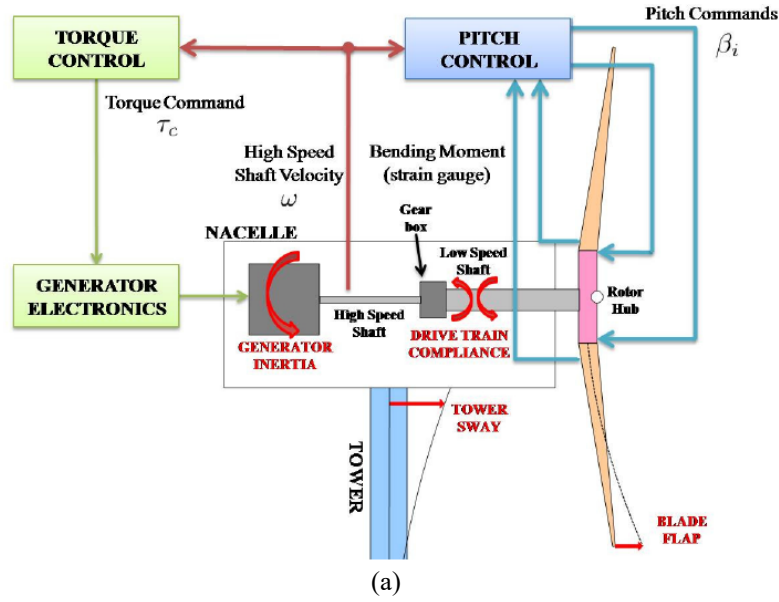


Figure III-16.2. (a) Scheme of the torque and pitch control strategies of a wind turbine [15] (b) Power curve of the NREL 5MW wind turbine

There are two main control loops to regulate the rotational speed of the wind turbine: The torque loop and the pitch loop. Each one of them is active in a different zone of the power curve. The torque loop, explained in detail in the work of Harris et al. [16], is active in the partial power zone of the power curve, plotted in blue color in Figure III-16.2 (b). On the other hand, in the rated power zone, plotted in red color in Figure III-16.2 (b), the objective is to reduce the power received by the wind turbine from the wind by means of the pitch control, explained in the work of Harris et al. [16].

The main control objective in the partial power zone is to maximize the power the wind turbine extracts from the wind, which can be expressed as in Eq. (III-16.1).

$$P_{opt} = \frac{1}{2} \cdot \rho \cdot C_p \cdot A \cdot v^3 \quad [W] \quad (III-16.1)$$

where  $\rho$  [kg/m<sup>3</sup>] is density of the air,  $C_p$  [-] is the power coefficient,  $A$  [m<sup>2</sup>] is the area covered by the rotor and  $v$  is the wind speed.

However, in order to express the real power the wind turbine extracts from the wind, the misalignment between the incident wind and the rotor must be considered, commonly known as the yaw angle. The expression is shown in Eq. (III-16.2).

$$P = P_{opt} \cdot \cos^3(\theta_{yaw}) \quad [W] \quad (III-16.2)$$

where  $\theta_{yaw}$  is the yaw angle.

163 As it can be observed in Eq. (III-16.2), a correct alignment of the wind turbine with the direction of the  
164 incident wind can make the power generated by the wind turbine increase considerably. The control system  
165 that allows a correct alignment of the wind turbine with respect to the incident wind is the yaw control. A  
166 detailed explanation about the yaw control system of a 5 kW wind turbine is introduced in the work of  
167 Yücel et al. [17]. Hence, an adequate design of the yaw control strategy of the wind turbine can be translated  
168 into a considerable increment of the power generated by the system.

169 On the other hand, as a result of the high inertia values of the mechanical components that participate in  
170 the yaw rotation, remarkable mechanical loads arise in different elements of the wind turbine. The physical  
171 effect that explains these loads is known as the gyroscopic effect. An study of possible control strategies  
172 aimed to attenuate the high mechanical loads resulting from the gyroscopic effect are presented in [18,19].  
173 Additionally, an analysis of the mechanical loads generated as a consequence of the yaw rotation is pre-  
174 sented in the work of Shariatpanah et al. [20].

175 As a result, an adequate design of the yaw control strategy allows not only maximization of the power  
176 generated by the wind turbine, but also reduction of the mechanical loads in several elements of the wind  
177 turbine, and, thus, to increment its lifetime.

178 The objectives of the proposed yaw control strategy are:

- 179 - Achieve a fully autonomous and self-tuning yaw control strategy to be implemented in the wind  
180 turbine.
- 181 - Design a control strategy based on ML that can continuously learns from its own experience.
- 182 - Selection of the optimal yaw control action (maximal power and minimal loads possible) for every  
183 possible scenario of the wind turbine operation.

184 The main applications of the designed yaw control strategy are:

- 185 - Increment of the power produced by the wind turbine, with the consequent enhancement of its effi-  
186 ciency, and the reduction of the LCOE.
- 187 - Reduction of the mechanical loads originated as a result of the yaw rotation, with the consequent  
188 increment of the lifetime of the mechanical components of the wind turbine, and the reduction of  
189 the LCOE.

190

191

### III-16.3. Machine Learning and Artificial Intelligence techniques

192 The AI is the science that studies the projection of the human intelligence in technological machines. In  
193 other words, the AI is the science that analyses the possibility to develop smart behavior patterns in tech-  
194 nological machines. The AI is considered to exist since the time of ancient Greek civilizations. In fact, there  
195 are Greek myths about mechanical systems designed to emulate the human behavior. Later, during 19th  
196 and 20th centuries, the development of the first computers is considered as an attempt to emulate the work-  
197 ing principle of the human brain in terms of calculations and memory. Nowadays, with the technological  
198 advances in the field of the informatics and the existence of very large amounts of data to be processed, the  
199 AI is on the focus of the research work.

200 The field of the AI is composed by numerous different techniques, which, in general, have been devel-  
201 oped to emulate the human intelligence or decision making capability, as it is explained in the work of  
202 Wang et al. [21]. The most important AI techniques are the RL, ANNs, Fuzzy Logic, bio-inspired or me-  
203 taheuristic optimization algorithms and Bayesian Networks. Each AI techniques serves to a determined  
204 goal and could be used individually or in interrelation with other AI techniques.

205 Bayesian Networks [22,23] are probability based networks that allow selection of the best action when  
206 a priori probabilities are known. Metaheuristic optimization algorithms [24,25] allow selection of the opti-  
207 mal action when the process is defined in a cost function. Bayesian Networks and optimization algorithms  
208 emulate the capability of the human brain to make decisions.

209 One of the most important features that offers the AI is the capability of the systems to learn automati-  
210 cally. This feature of self-learning is commonly known as ML, as it is explained in detail in the work of  
211 Fadlullah et al. [26]. The ML has undergone an important boom after the development of the ANNs, which  
212 are able to continuously learn from very large amounts of data. RL is another type of ML, in which the  
213 systems learns to make the best decisions in a given environment by using its own experience.

214 With the technological boom and the increasing processing capability of the processors a new learning  
215 method known as Deep Learning [26] has been born, in which new and amplified configurations of ANNs  
216 are used for the ML process. In the same way, the Deep Reinforcement Learning [26] method has also been

217 created, which combines the use of the RL algorithm and ANNs to store the matrix  $Q(s,a)$  related to the RL  
218 algorithm.

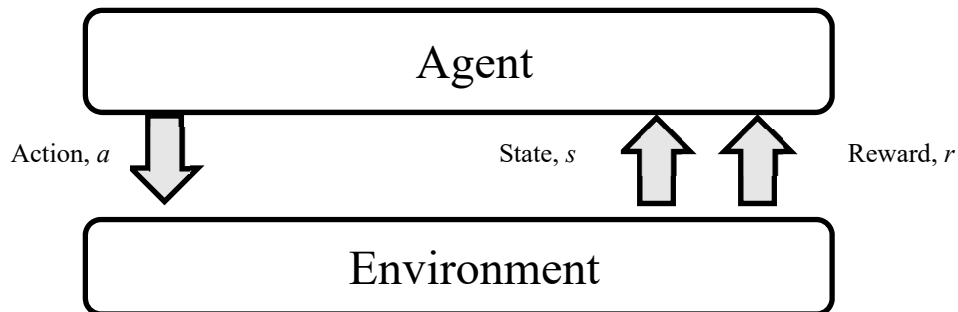
219 The AI has numerous applications nowadays. Optimization algorithms are widely used in the business  
220 and public sectors due to their good results to reduce costs and increase gain margins [27]. Big companies  
221 like Amazon use predictions based on online searches and ML to carry out market studies and maximize  
222 their profits. The application SIRI of Apple brand mobile phones is a digital personal assistant that uses  
223 ML techniques to continuously self-learn. RL techniques are used in different fields such as the continuous  
224 learning of manufacturing robots, in Fanuc for instance, or to predict optimal trading strategies in the fi-  
225 nancial sector.

226 The self-tuning ML based yaw control strategy presented in this chapter makes use of three different AI  
227 techniques: RL, ANN and metaheuristic optimization algorithms. This section is structured as follows: the  
228 theoretical background of the RL is explained in Subsection III-16.3.1. Subsection III-16.3.2 analyses the  
229 theory behind the ANNs. And, finally, the theoretical basis of the optimization algorithms is introduced in  
230 the Subsection III-16.3.3.

### 231 III-16.3.1. Reinforcement Learning

232 RL [10,28-30] is an AI technique, corresponding to a type of ML, in which a determined system learns  
233 from the experience of its own interaction with the environment in which it is placed. As it is stated in the  
234 work of Sutton et al. [28], the training process of a RL algorithm is achieved by trial and error with the  
235 objective of maximizing a reward function defined numerically and by mapping of situations to actions.

236 A pipeline with the basic operating principle of a RL algorithm is presented in Figure III-16.3. A defined  
237 agent which is in a determined environment receives information of its state ( $s \in S$ ) and decides to take the  
238 action ( $a \in A$ ). As a result of this action, the agent receives information of its new state and the immediate  
239 reward of the action ( $r \in R$ ). The objective of the RL algorithm is to find a map of states to actions, known  
240 as policy, to maximize the long-term reward in different situations. In other words, the RL controller selects  
241 the future actions with regard to the experiences of a whole range of actions in predefined states. The ex-  
242 periences are obtained by trial and error by interaction with a dynamic environment, as exposed in the work  
243 of Kaelbling et al. [31].  
244



245

246 *Figure III-16.3. Basic pipeline of a RL algorithm [12]*

247 The main elements of a RL algorithm are:

- 248 - State ( $s \in S$ ): Defines the state of an agent that is placed in a determined environment.
- 249 - Action ( $a \in A$ ): Defines the action taken by an agent that is in a defined state ( $s \in S$ ) in a determined  
250 environment.
- 251 - Reward ( $r \in R$ ): Defines the immediate reward received by an agent that takes a certain action ( $a \in A$ )  
252 in a given state ( $s \in S$ ).
- 253 - Policy ( $\pi$ ): It is a mapping of the actions ( $a \in A$ ) to the states ( $s \in S$ ). Thus, it defines the behavior  
254 of the agent.
- 255 - Long-term reward ( $R_t$ ): Indicates the long term reward received by the agent if a certain action ( $a \in A$ )  
256 in a given state ( $s \in S$ ) is taken. The long-term reward is the value to be maximized.

257 The long-term reward  $R_t$  of a RL algorithm can be numerically calculated in different ways. The most  
258 widely-used expression is based on the addition of the immediate rewards ( $r \in R$ ) received by the agent  
259 during a determined period of time and using a discount factor  $\gamma$ , as it is shown in Eq. (III-16.3).

$$R_t = \sum_{k=t}^{t+T} \gamma_k \cdot r_{t+k+1} \quad (III-16.3)$$

260 where the discount factor  $\gamma$  is set to  $0 < \gamma < 1$ .

261 From now on, in order to refer to the function that indicates the long-term reward  $R_t$  expected by the  
 262 agent a new expression is shown in Eq. (III-16.4).

$$E \left( \sum_{k=t}^{t+T} \gamma_k \cdot r_{t+k+1} \right) \quad (III-16.4)$$

263 One important aspect related to the RL algorithms is that the environment in which the agent is placed  
 264 is defined as a Markov Decision Process (MDP). This means that the environment transitions are independ-  
 265 ent on past states and exclusively depend on the current state ( $s \in S$ ) and the action taken ( $a \in A$ ). There-  
 266 fore, the expressions of the state and reward transitions are presented in Eq (III-16.5) and Eq. (III-16.6),  
 267 respectively.

$$p_{ss'}^a = p \{s_{t+1} = s' | s_t = s, a_t = a\} \quad (III-16.5)$$

$$R_{ss'}^a = E \{r_{t+1} | s_t = s, a_t = a, s_{t+1} = s'\} \quad (III-16.6)$$

268 The policy  $\pi$  followed by the agent defines the mapping of actions to states and, thus, dictates the criteria  
 269 to take determined actions. Hence, the policy  $\pi$  defines the probability to select each action ( $a \in A$ ) in each  
 270 determined state ( $s \in S$ ). As a result, the expected long-term reward with respect to the current state ( $s \in$   
 271  $S$ ) and the policy  $\pi$  followed, known as  $V^\pi(s)$ , and the expected long-term reward with respect to the  
 272 current state ( $s \in S$ ), the current action ( $a \in A$ ) and the policy  $\pi$  followed, known as  $Q^\pi(s, a)$ , can be  
 273 numerically calculated as shown in Eq. (III-16.7) and Eq. (III-16.8), respectively.

$$V^\pi(s) = E_\pi \{R_t | s_t = s\} = E_\pi \left\{ \sum_{k=t}^{t+T} \gamma_k \cdot r_{t+k+1} | s_t = s \right\} \quad (III-16.7)$$

$$Q^\pi(s, a) = E_\pi \{R_t | s_t = s, a_t = a\} = E_\pi \left\{ \sum_{k=t}^{t+T} \gamma_k \cdot r_{t+k+1} | s_t = s, a_t = a \right\} \quad (III-16.8)$$

274 The optimal values of both  $V^\pi(s)$  and  $Q^\pi(s, a)$  can be expressed as in Eq. (III-16.9) and Eq. (III-16.10).

$$V(s) = \max(V^\pi(s)) \quad (III-16.9)$$

$$Q(s, a) = \max(Q^\pi(s, a)) \quad (III-16.10)$$

275 The objective of the RL algorithm is to find the optimal mapping of actions to states so that the value of  
 276 the  $Q(s, a)$  expressed in Eq. (III-16.10) is maximized for each par of state ( $s \in S$ ) and action ( $a \in A$ ). To  
 277 that end, there are 3 different methods to solve a MDP process: Dynamic Programming (DP), Monte Carlo  
 278 (MC) method and Temporal Differences (TD). In the following lines an explanation on each one of them  
 279 is introduced.

### 280 - Dynamic Programming

281 The DP method, explained in detail in the works of Bertsek et al. [32-34], is based on the knowledge of  
 282 a model of the environment in which the agent is placed. That means that the state transitions  $p_{ss'}^a$ , see Eq.  
 283 (III-16.5), and the reward transitions  $R_{ss'}^a$ , see Eq. (III-16.6), can be calculated analytically. As a result, the  
 284 value of  $V^\pi(s)$  and  $Q^\pi(s, a)$  can also be represented analytically using Bellman equations, as shown in Eq.  
 285 (III-16.11) and Eq. (III-16.12).

$$\begin{aligned} V^\pi(s) &= E_\pi \{r_{t+1} + \gamma \cdot V^\pi(s_{t+1}) | s_t = s\} \\ &= \sum_a \pi(s, a) \sum_{s_{t+1}} p_{ss'}^a \cdot [R_{ss'}^a + \gamma \cdot V^\pi(s_{t+1})] \end{aligned} \quad (III-16.11)$$

$$\begin{aligned}
 Q^\pi(s, a) &= E_\pi \{ r_{t+1} + \gamma \cdot Q^\pi(s_{t+1}, a_{t+1}) \mid s_t = s, a_t = a \} \\
 &= \sum_a \pi(s, a) \sum_{s_{t+1}} p_{ss'}^a \cdot [R_{ss'}^a + \gamma \cdot Q^\pi(s_{t+1}, a_{t+1})]
 \end{aligned}
 \tag{III-16.12}$$

286 The numerically calculated values of  $V^\pi(s)$  and  $Q^\pi(s, a)$  are used to perform an iterative algorithm in  
 287 which every action ( $a \in A$ ) of every possible state ( $s \in S$ ) is considered and the policies  $\pi$  that maximize  
 288 the value of  $Q(s, a)$  are to be found.

289 One of the biggest drawbacks of this method is the computational cost, since for the calculation of each  
 290 policy  $\pi$  calculations related to a great number of states and actions have to be performed. A pseudocode  
 291 of the DP algorithm is presented in Algorithm III-16.1.  
 292

---

#### Dynamic Programming algorithm

---

```

% Initialize Q(s,a) randomly
Q(s,a) = Q(s,a)_ini
% Start the DP algorithm
while ( $\Delta > \beta$ ) do
% Initialize the minimum Q(s,a) improvement
 $\Delta = 0$ 
% Define the actual state and select an action
s  $\leftarrow$  ( $s \in S$ )
a  $\leftarrow$  ( $a \in A$ )
% Calculate Q(s,a)
Q(s,a)  $\leftarrow$  Eq. (III-16.12)
% Calculate the Q(s,a) improvement
 $\Delta = \text{abs}(Q\_ant(s,a) - Q(s,a))$ 
Q_ant(s,a) = Q(s,a)
end

```

293 *Algorithm III-16.1. Pseudocode of a DP based RL algorithm*

#### 294 - Monte Carlo method

295 The MC method [35,36] is based on the assumption that a model of the environment is unknown, and  
 296 thus, its performance depends on the experimental data. Since the model is unknown, the values of the state  
 297 transitions  $p_{ss'}^a$ , see Eq. (III-16.5), and the reward transitions  $R_{ss'}^a$ , see Eq. (III-16.6), and as a result, the  
 298 values of  $V^\pi(s)$  and  $Q^\pi(s, a)$  cannot be analytically computed, so they are calculated as an average of the  
 299 experimentally obtained reward values.

300 The objective is to try to calculate the value of  $Q^\pi(s, a)$  for all the state-action pairs and find the policies  
 301  $\pi$  that maximize the value of  $Q(s, a)$ . To that end, usually stochastic policies that have probabilities greater  
 302 than 0 to consider each state ( $s \in S$ ) and action ( $a \in A$ ) are implemented.

303 Different MC based algorithms can be implemented:

- 304 ○ Off-policy algorithms: The calculated policies are simultaneously used for the control  
 305 strategy implemented in the system.
- 306 ○ On-policy algorithms: The policies calculated by the ongoing MC algorithm and the pol-  
 307 icies used by the control strategy implemented in the system are separated.

308 A pseudocode of the DP algorithm is presented in **¡Error! No se encuentra el origen de la referencia..**  
 309  
 310  
 311  
 312  
 313  
 314  
 315  
 316



---

**Monte Carlo algorithm**

---

```

% Define a policy  $\pi$  and select an episode
% For each state  $s$  select an action  $a$ 
 $s \leftarrow (s \in S)$ 
 $a \leftarrow (a \in A)$ 
% Calculate the long term reward  $R_t$ 
 $R_t \leftarrow \text{Eq. (III-16.3)}$ 
 $R_t\_vec = [R_t\_vec, R_t]$ 
% Calculate  $Q(s,a)$  as a weighted average
 $Q(s,a) = \text{average}(R_t\_vec)$ 
% Evaluate the policy  $\pi$ 

```

---

317 *Algorithm III-16.2. Pseudocode of a MC method based RL algorithm*

318 - Temporal Differences

319 The TD method is a combination of DP and MC methods having the advantages associated to each one  
320 of them. It is based on analytical calculation, like the DP method, but, like the MC method, it does not  
321 depend on a model of the environment. In this method, the calculations to continuously learn are performed  
322 between successive predictions instead of between predictions and the final value. Hence, the convergence  
323 is faster and the computational cost is remarkably reduced. The two principal TD based algorithms are Q-  
324 Learning, explained in detail in the works of Watkins et al. [7,37], and SARSA, introduced in the work of  
325 Adam et al. [38].

326 The principal difference between both methods is the calculation of the values of  $Q(s,a)$ . In the Q-Learn-  
327 ing algorithm the state and actions are quantified and a matrix is obtained as a result of mapping a  $Q(s,a)$   
328 value to each state-action par. However, in SARSA, the function  $Q(s,a)$  is considered as an exponential  
329 moving average continuous function.

330 The calculation of the  $Q(s,a)$  in SARSA algorithm can be expressed as shown in Eq. (III-16.13).

$$Q(s_t, a_t) = Q(s_t, a_t) + \alpha \cdot [r + \gamma \cdot Q(s_{t+1}, a_{t+1}) - Q(s_t, a_t)] \quad (III-16.13)$$

331 The calculation of the  $Q(s,a)$  in Q-Learning algorithm can be expressed as shown in Eq. (III-16.14).

$$Q(s_t, a_t) = Q(s_t, a_t) + \alpha \cdot [r + \gamma \cdot \max_a Q(s_{t+1}, a_{t+1}) - Q(s_t, a_t)] \quad (III-16.14)$$

332 A simplified pseudocode of the SARSA and Q-Learning algorithms is presented in ;**Error! No se en-**  
333 **cuentra el origen de la referencia..**

334

---

**SARSA algorithm**

---

```

% Initialize  $Q(s,a)$  randomly
 $Q(s,a) = Q(s,a)\_ini$ 
% Start the SARSA algorithm
while ( $s \in \text{Episode}$ ) do
% Define the actual state and select an action
 $s \leftarrow (s \in S)$ 
 $a \leftarrow (a \in A)$ 
% Observe  $r$  and  $s_{t+1}$ 
% Define the next action
 $a_{t+1} \leftarrow (a \in A)$ 
% Calculate  $Q$ 
 $Q(s,a) \leftarrow \text{Eq. (III-16.13)}$ 
 $s = s_{t+1}$ 
% Evaluate the policy  $\pi$ 
end

```

---

**Q-Learning algorithm**

---

```

% Initialize  $Q(s,a)$  randomly
 $Q(s,a) = Q(s,a)\_ini$ 
% Start the Q-Learning algorithm
while ( $s \in \text{Episode}$ ) do
% Define the actual state and select an action
 $s \leftarrow (s \in S)$ 
 $a \leftarrow (a \in A)$ 
% Observe  $r$  and  $s_{t+1}$ 
% Define the next action
 $a_{t+1} \leftarrow (a \in A)$ 
% Calculate  $Q$ 
 $Q(s,a) \leftarrow \text{Eq. (III-16.14)}$ 
 $s = s_{t+1}$ 
% Evaluate the policy  $\pi$ 
end

```

---

335

(a)

(b)

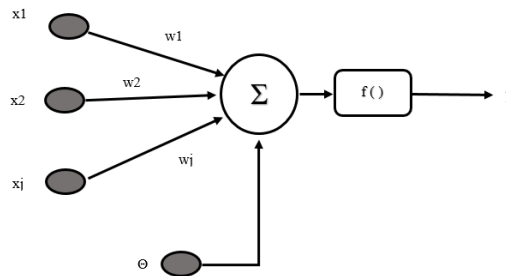
336 Algorithm III-16.3. (a) Pseudocode of a SARSA based RL algorithm (b) Pseudocode of a Q-Learning based RL  
337 algorithm

### 338 III-16.3.2. Artificial Neural Networks

339 ANNs correspond to a branch of the AI intended to mimic the performance of a biological brain. Bio-  
340 logical brains are composed by millions of neurons distributed in layers and widely interconnected between  
341 them. Through these interactions between neurons the information flow from one neuron to another occurs.  
342 Furthermore, the information flow happens always in one direction, which can be either forwards or back-  
343 wards. ANNs [39-41], which try to emulate this behavior, are digital systems with a variable number of  
344 neurons distributed in a structure similar to that of biological networks and with a similar functionality.

345 According to the work of Yang [42], the first standard artificial neuron design was introduced by W.  
346 McCulloch and W. Pitts in 1943 and, after that, they have undergone an important development. Nowadays  
347 they are very precious especially for their good performance in parallel processing, distributed memory  
348 alongside the number of neurons and the adaptability to the environment and the generalization capability.

349 ANNs are a compound of a variable number of neurons distributed in different ways and with a different  
350 type of interconnections. An individual neuron, shown in Figure III-16.4, is the smallest element of an ANN  
351 and presents the following structure:  
352



353 Figure III-16.4. Neuron of an ANN

355 The main elements of an artificial neuron are:

- 356 - Inputs ( $x_j$ ): Define the inputs to the neuron.
- 357 - Input weights ( $w_j$ ): Define the weights of each input to the neuron.
- 358 - Propagation rule ( $h_i$ ): It defines the combination of the different inputs of the neuron before the  
359 activation function. The most common propagation rule is the linear combination of the product of  
360 each input and its weight. Moreover, usually another parameter commonly expressed as  $\theta$  is added.  
361 Therefore, the propagation rule can be mathematically expressed as shown in Eq. (III-16.15).

$$h(x_1, \dots, x_j, w_1, \dots, w_j) = \sum_{j=1}^n w_j \cdot x_j - \theta \quad (III-16.15)$$

- 362 - Activation function ( $f_i$ ): The activation function defines the activation state of the neuron. Addi-  
363 tionally, it represents the output of the neuron.

364 If it is an on/off neuron, the activation function of the neuron can be expressed as in Eq. (III-16.16).  
365 The output of this neuron is discrete, and corresponds to the original one introduced by W. McCul-  
366 loch and W. Pitts in 1943.

$$y = \begin{cases} 1 & \text{if } \sum_{j=1}^n w_j \cdot x_j \geq \theta \\ 0 & \text{if } \sum_{j=1}^n w_j \cdot x_j < \theta \end{cases} \quad (III-16.16)$$

367 However, when a continuous output of the neuron is desired, usually a sigmoid function [43] is used  
 368 as the activation function, as shown in Eq. (III-16.17).

$$f(x) = \frac{1}{1 + e^{-\beta \cdot x}} \quad (III-16.17)$$

369 where the value associated to the exponential factor is  $\beta > 0$ .

370 ANNs are formed by compound of a variable number of neurons in different structures and interconnec-  
 371 tion patterns. The neurons are divided in layers. As it is shown in Figure III-16.5, usually in a standard  
 372 ANN there are 3 different neuron layers: The input layer (contains the input neurons, which are in number  
 373 the same as the inputs of the ANN), the hidden layer (contains the processing neurons) and the output layer  
 374 (contains the output neurons, which are in number the same as the outputs of the ANN). The number of  
 375 hidden layers and the number of neurons in each hidden layer is adaptable and can be modified by the  
 376 designer of the ANN.

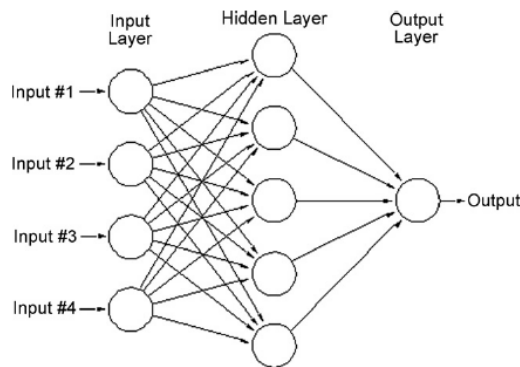
377 There are different types of ANNs. The classification can be done according to different factors:

378 According to the number of layers:

- 379 - Simple layer: ANNs with only one neuron layer.
- 380 - MultiLayer: ANNs with the neurons distributed in more than one layer.

381 According to the information flow:

- 382 - Feedforward: The information flow occurs exclusively in the direction from the input layer to the  
 383 output layer. One example of this architecture is the MultiLayer Perceptron.
- 384 - Feedback or recurrent: There is information flow in both directions, i.e., from the input layer to the  
 385 output layer and from the output layer to the input layer direction. One example of this architecture  
 386 is the NonLinear Autoregressive Neural Network.



387  
 388 *Figure III-16.5. Layer based structure of an ANN [44]*

389 The training algorithms of the ANNs are the responsible for making the ANN learn from its input values.  
 390 There are two main ANN training method groups: The supervised learning and the unsupervised learning.  
 391 As it is exposed in the work of Chen et al. [39], the supervised learning adjusts the values of the weights  
 392 related to the interconnection between neurons with the objective of minimizing the error existent between  
 393 the output of the ANN and the reference output. That means that a reference output for the ANN should be  
 394 known in the case of a supervised learning. The most important application of the supervised learning is  
 395 for regressions or modelling of systems. One of the most used examples of supervised learning is the Back-  
 396 Propagation algorithm.

397 The unsupervised learning do not need an output reference and the ANN is trained with numerous input  
 398 patterns to explore the relation between them and categorize them. The most important application of the  
 399 unsupervised learning is the clustering of data. A combination of supervised and unsupervised learning  
 400 methods in an hybrid learning strategy is also possible.

### 401 **III-16.3.3. Optimization Algorithms**

402 Optimization algorithms are techniques designed and aimed to find the maximum/minimum or optimal  
 403 solution of a determined function or problem. First optimization algorithms were introduced in the 20<sup>th</sup>

404 century. Nowadays, optimization algorithms are applied to a grand variety of applications. As it is explained  
 405 in the work of Yang et al. [42], one of the biggest application fields of the optimizations algorithms is the  
 406 industrial engineering world, where the reduction of costs, the increment of the efficiency and the optimi-  
 407 zation of the industrial processes have become of capital importance.

408 Among the advantages of the optimization algorithms is the existence of processors with high capacity  
 409 that allow the execution of the optimization algorithms at a considerable speed. The main drawback of the  
 410 optimization algorithms is the necessity to have reliable models of the process that is to be optimized.

411 There are several types of optimization algorithms. In the work of Yang et al. [42], a classification of  
 412 the optimization algorithms is proposed:

413 According to the existence of derivatives in the algorithm:

414 - Gradient based: They have derivatives in their optimization code. For instance, Gauss-Newton  
 415 methods belong to this group.

416 - Gradient-free: They do not have derivatives in their optimization code. For example, the Nelder-  
 417 Mead downhill simplex method belongs to this group.

418 According to the existence of randomness in the algorithm:

419 - Deterministic: There is no randomness in the optimization code. The result is always the same if the  
 420 initial point is the same. An example of a deterministic optimization algorithm is the Hill climbing  
 421 algorithm without random start.

422 - Stochastic: There is randomness in the optimization code. Hence, the result is not always the same  
 423 even if the initial point is the same. An example of a stochastic optimization algorithm is the Genetic  
 424 Algorithm (GA).

425 According to the mobility:

426 - Local: They typically converge to local optima because they do not have the ability to escape from  
 427 them as a result of the lack of randomness in the optimization code. They are usually deterministic  
 428 algorithms.

429 - Global: They always try to find the global optima. They have the ability to escape local optima as a  
 430 result of the randomness in the optimization code. They are usually stochastic algorithms.

431 An important group inside the optimization algorithms is the bio-inspired or metaheuristics algorithms,  
 432 which are inspired in natural processes to solve optimization problems. The metaheuristic algorithms [45-  
 433 47] have been widely studied in the literature. There are many metaheuristic algorithms: Ant algorithm  
 434 [48], bee algorithm [49], simulated annealing [50], GA, PSO, Differential Evolution (DE), etc.

435 The most widely used metaheuristic optimization algorithms are introduced in the following lines.

436

437 - Genetic Algorithms

438 The GAs [51,52] are metaheuristic optimization algorithms inspired in the evolution of biological indi-  
 439 viduals proposed by Charles Darwin. The GAs were first developed by Holland [53] during the decades of  
 440 the 1960s and the 1970s.

441 As it is explained in detail in the work of Wang et al. [45], a GA is formed by a population of chromo-  
 442 somes or individuals, each one of them representing a solution to the optimization problem. Additionally,  
 443 a fitness/cost function that evaluates each one of the individuals and provide them with a fitness value is  
 444 necessary. The fitness function evaluates the specification fulfillment corresponding to each one of the  
 445 individuals and, thus, the fitness value is an indicator of the chances of survival and reproduction of each  
 446 one of the individuals. As a result, the individuals with the best fitness value tend to survive and the algo-  
 447 rithm evolves towards the optimal solutions.

448 The execution of a GA could be summarized in the following 5 steps:

449 1) Initialization. Traditionally, the population is formed by a group of randomly generated individual  
 450 solutions.

451 2) Evaluation. The fitness of each individual in the population is evaluated.

452 3) Selection. Individuals are selected based on the fitness value to breed a new generation.

453 4) Evolution. New individuals are created through crossover and mutation operations. The new popula-  
 454 tion is composed of the individuals in the new generation and a few individuals from the previous genera-  
 455 tion.

456 5) Termination. Steps 2 to 4 are repeated until a termination condition has been reached.  
457

458 - Particle Swarm Optimization

459 The PSO [54] algorithms are metaheuristic optimization algorithms inspired in the behavior of a group  
460 of particles, referred as swarm, in a search space and evolving towards an optimal solution. As it is  
461 explained in the work of Wang et al. [46], this algorithm is widely used due to its high robustness, small  
462 number of tunable parameters and its easy implementation.

463 As introduced in the work of Khan et al. [46], each particle is a possible solution to the optimization  
464 problem, and is associated with a position vector  $x_{i,t}$  and a velocity vector  $v_{i,t}$ . Exactly as in the case of the  
465 GAs, in a PSO algorithm there must be a fitness function that evaluates the specification fulfillment of each  
466 particle and provides them with a fitness values.

467 The velocity and position update of each particle is calculated with the following expressions presented  
468 in Eq. (III-16.18) and Eq. (III-16.19), respectively.

$$v_{i,t+1} = H \cdot v_{i,t} + \varphi_1 \cdot (x_{opt_{i,t}} - x_{i,t}) + \varphi_2 \cdot (x_{global\_opt_{i,t}} - x_{i,t}) \quad (III-16.18)$$

$$x_{i,t+1} = x_{i,t} + v_{i,t+1} \cdot \Delta t \quad (III-16.19)$$

469 where  $H$  [ $\text{kg} \cdot \text{m}^2$ ] is the inertia constant of the system,  $\varphi_1$  [-] is the exploitation factor,  $\varphi_2$  [-] is the  
470 exploration factor,  $x_{opt_{i,t}}$  [m] is the best solution of the particle and  $x_{global\_opt_{i,t}}$  [m] is the best solu-  
471 tion of the whole swarm.

472 As it can be observed in Eq. (III-16.18), the velocity of each particle is computed with regard to the  
473 personal best fitness obtained by that particle and the global best fitness obtained by the whole swarm. By  
474 modifying factors  $\varphi_1$  [-] and  $\varphi_2$  [-] the exploration and exploitation capability of the algorithm can be  
475 configured. Furthermore, the inertia constant  $H$  [ $\text{kg} \cdot \text{m}^2$ ] defines the movement capacity of the particles.

476 The execution of a PSO could be summarized in the following 5 steps:

- 477 1) Initialization. The swarm population is randomly formed.  
478 2) Evaluation. The fitness of each individual particle is evaluated.  
479 3) Modification. The best position of each particle, the best position of the whole swarm and each par-  
480 ticle's velocity are computed.  
481 4) Update. Move each particle to the new position.  
482 5) Termination. Steps 2 to 4 are repeated until a termination condition has been satisfied.  
483

484 - Differential Evolution

485 The DE algorithm is metaheuristic optimization algorithm inspired in the evolutionary principles and  
486 intended to solve global optimization problems. The original DE algorithm was first introduced in the work  
487 of Storn and Price [55]. The DE algorithm starts with randomly initialized solution vectors, and like the  
488 GA algorithm is based on the principles of mutation, crossover and selection. Nevertheless, in contrast to  
489 GAs, the DE algorithms operate over each dimension of the solution separately.

490 The mutation is based on the recombination of three randomly chosen vectors, as shown in Eq. (III-  
491 16.20).

$$v_{i,t+1} = x_{a,t} + T \cdot (x_{b,t} - x_{c,t}) \quad (III-16.20)$$

492 where  $T \in [0,2]$  is commonly known as the differential weight and is a parameter adjustable by the  
493 designer.

494 After the mutation a crossover stage based on the crossover probability  $C_r \in [0,1]$  is performed and the  
495 fitness of the individuals is evaluated. The selection stage is based on the fitness value of each individual,  
496 exactly as in the case of the GAs.

497 The execution of a DE algorithm could be summarized in the following 5 steps:

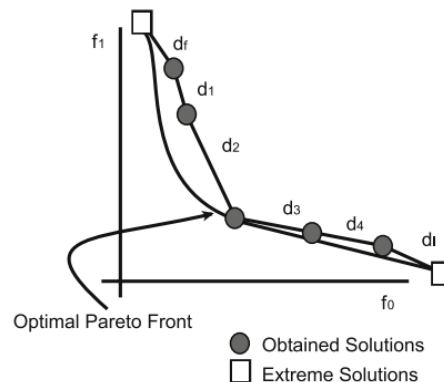
- 498 1) Initialization. Traditionally, the population is formed by a group of randomly generated individual  
499 solutions.  
500 2) Mutation. The mutation shown in Eq. (III-16.20) is performed.  
501 3) Crossover. The individual of the new generation are formed based on the crossover probability.  
502 4) Selection. The individuals are selected based on their fitness value to breed a new generation

503 5) Termination. Steps 2 to 4 are repeated until a termination condition has been reached.  
504

505 - Multiobjective optimization. Pareto optimal Front

506 A multiobjective optimization [56-58] problem is that in which more than one objective is to be opti-  
507 mized. In contrast to single-objective optimization problems, in multiobjective cases there is not only one  
508 unique optimal solution, but a set of optimal solutions that respond to the trade-off or compromise necessity  
509 between the objectives to be optimized.

510 The concept of optimization of multiobjective problems was generalized in the work of Vilfredo Pareto  
511 [59] in 1896. In these type of problems a solution is dominated if there is any other solution that has a better  
512 (higher or lower depending on the context of the optimization problem) fitness value for all the objectives  
513 to be optimized. If there is no such a solution, i.e., if the improvement of one objective causes the degrading  
514 of any other objective, then the solution is known as non-dominated. The set of non-dominated solutions is  
515 known as the Pareto optimal Front (PoF). A PoF of a double-objective optimization problem is illustrated  
516 in Figure III-16.6.



517  
518

Figure III-16.6. PoF of a double-objective optimization problem [57]

519 As it can be observed in Figure III-16.6, all the points forming the continuous line marked as the PoF  
520 respond to the same principle of compromise necessity between the objectives. If the value of one of the  
521 objectives is improved, the other one degrades. An algorithm to find the PoF of a multiobjective problem  
522 could be implemented in any of the previously presented metaheuristic optimization algorithms.  
523

### 524 III-16.4. Machine Learning based wind turbine yaw control

525 An adequate alignment of the wind turbine rotor with respect to the incoming wind by means of the yaw  
526 system of the wind turbine enables increment of the power generation. Nevertheless, as it was exposed in  
527 Section III-16.2 of this chapter, the enhancement of the generated power is achieved at cost of an increase  
528 of the mechanical loads in different elements of the wind turbine, especially the yaw bearings. Hence, an  
529 adequate design and tuning of the yaw control system is of great importance to both optimize the power  
530 generation of the wind turbine and ensure its safe operation. The absence of an adequate control strategy  
531 could result in an excessively aggressive yaw activity, which could endanger the safety of the mechanical  
532 components of the wind turbine and reduce their lifetime.

533 Usually, classical control structures based on PIDs have been used for the design of the yaw control  
534 strategy of the wind turbine [20,60]. However, these classical control structures show some drawbacks in  
535 form of “wind up” of the integral action and posterior big oscillations, which can result in an undesired  
536 increment of the mechanical loads. As a result, some advanced control strategies for the yaw angle control  
537 of a wind turbine are proposed in the literature. In this context, Song et al. [61] present a control strategy  
538 based on a Model Predictive Control and Bharani et al. [62] introduce a Fuzzy Logic based control strategy  
539 for this purpose. In the work of Saenz-Aguirre et al. [12], an ANN based RL control strategy is proposed  
540 for the yaw control of a wind turbine.

541 In this chapter, with the objective of achieving an improved performance of the yaw control system of a  
542 wind turbine, a ML based wind turbine yaw control system is exposed. A block diagram of the proposed  
543 ML based yaw control strategy is presented in Figure III-16.7.  
544

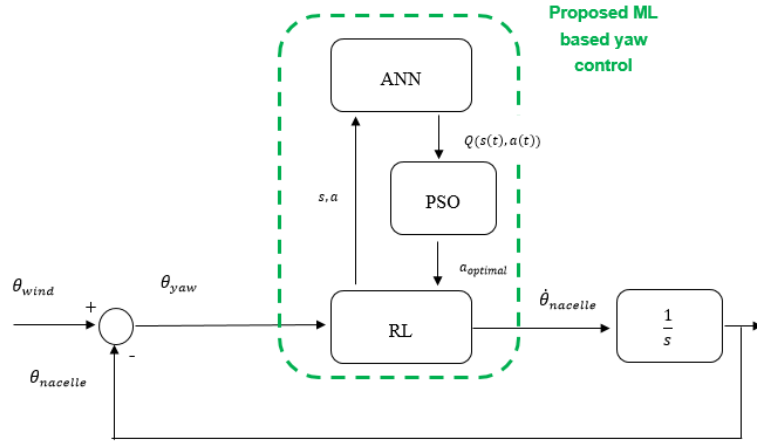


Figure III-16.7. Pipeline of the proposed ML based yaw control

The proposed yaw control system is based on the following AI techniques:

- A RL algorithm that learns from its own experience and enables the wind turbine to select the optimal decision in each scenario of its operation.
- An ANN to store the data of the matrix  $Q(s,a)$  of the RL algorithm.
- A PSO and PoF based optimization algorithm to select the set of optimal actions that respond to the compromise necessity between the power increment and the mechanical loads associated to the yaw rotation.

This section is structured as follows: the design procedure of the RL algorithm applied to the ML based yaw control is explained in Subsection III-16.4.1. Subsection III-16.4.2 presents the structure and design process of the MLP-BP neural network. The design of the PSO and PoF based algorithm is explained in Subsection III-16.4.3. Finally, the Decision Making (DM) algorithm is exposed in Subsection III-16.4.4.

### III-16.4.1. Yaw Control RL

The RL algorithm developed for the yaw control of a HAWT presents multiple state, action and immediate reward variables. The objective of the multivariable structure is an improved characterization of the system in the most accurate way possible. To that end, 2 state variables, 2 action variables and 2 immediate reward variables are considered in the proposed RL algorithm.

The states  $s$  are:

- StateYawA [deg]: This state defines the orientation difference between the wind incident to the rotor and the nacelle of the wind turbine. As it can be observed in Eq. (III-16.2), the power output of the wind turbine is affected by this misalignment angle. The expression to calculate the value of this state is shown in Eq. (III-16.21).

$$\theta_{yaw} = \theta_{wind} - \theta_{nacelle} \quad (III-16.21)$$

- StateWindS [m/s]: This state defines the wind speed value incident to the rotor. As it has been shown stated in Figure III-16.2 (b), the power output of the wind turbine is not directly proportional to the wind speed value, but it depends on the operation zone of the wind turbine, which depends on the wind speed value. As a result, it is important to know the wind speed value because it will help characterize the possible power gain achievable with the yaw rotation of the wind turbine.

The actions  $a$  are:

- ActionYawK [deg/s]: This action defines the proportional gain associated to the yaw rotational speed controller. The expression to calculate the yaw rotational speed is shown in Eq. (III-16.22).

$$\Omega_{yaw} = ActionYawK \cdot \theta_{yaw} \quad (III-16.22)$$

As it can be seen in Eq. Eq. (III-16.22), the higher the value of the action ActionYawK [deg/s] is, the higher the yaw rotational speed will be.

- 578 - ActionYaw [deg]: This action defines the limit associated to the yaw rotation. In some cases, due to  
 579 mechanical actuator problem or safety issues, the yaw rotation of the nacelle is limited to a certain  
 580 value. The expression to note the rotation range allowed by this action is shown in Eq. (III-16.23).

$$\Delta\theta_{yaw} \in [-\text{ActionYaw}, \text{ActionYaw}] \quad (\text{III-16.23})$$

581 The immediate rewards  $r$  are:

- 582 - RewardP [%]: This immediate reward defines the power gain achieved by the wind turbine when a  
 583 certain yaw action is performed. The expression to compute this immediate reward is shown in Eq.  
 584 (III-16.24).

$$\text{RewardP} = \frac{P_{\text{control}} - P_{\text{no\_control}}}{P_{\text{no\_deviation}}} \cdot 100 \quad (\text{III-16.24})$$

585 As it can be observed in Eq. (III-16.24), in order to calculate the power gain 3 different scenarios  
 586 related to the yaw actuation of the wind turbine are considered. The scenario  $P_{\text{control}}$  refers to the  
 587 scenario in which the yaw control of the wind turbine is active and the nacelle of the wind turbine  
 588 rotates to the yaw command provided by the yaw control and at the provided yaw speed value. The  
 589 scenario,  $P_{\text{no\_control}}$  refers to the scenario in which the yaw control of the wind turbine is not  
 590 active, and, thus, the orientation of the wind turbine nacelle is fixed. Finally, the scenario  $P_{\text{no\_de-}}$   
 591  $\text{viation}$  refers to the scenario in which the nacelle of the wind turbine is perfectly aligned with the  
 592 direction of the wind incoming to the rotor. Hence, this value refers to the maximum power that the  
 593 wind turbine can generate with a defined value of the wind speed.

- 594 - RewardM [N·m]: This immediate reward defines the value of the mechanical moment in the yaw  
 595 bearings. The value of this immediate reward has been defined with the mechanical moment in the  
 596 yaw bearings because it has been found as the most critical mechanical load when performing a yaw  
 597 rotation. Different mechanical load values, or even a weighted average of them, could be considered  
 598 as the immediate reward to be considered by the proposed ML based yaw control algorithm.

599 As it was stated in Subsection III-16.3.1 of this chapter, in a RL algorithm the calculation of the values  
 600  $Q(s,a)$  for each state-action pair is associated to the long-term reward considering a discount factor  $\gamma$ , see  
 601 Eq. (III-16.3). In the RL algorithm proposed in this chapter there are 2 different immediate rewards  $r$ .  
 602 Therefore, 2 different matrices  $Q(s,a)$  will result in the algorithm. The expression to calculate the matrices  
 603  $Q(s,a)$  using the immediate rewards  $r$  is shown in Eq. (III-16.25).

$$Q(s, a) = \sum_{i=0}^{i=T} r_{t+i} \cdot \gamma^i \quad (\text{III-16.25})$$

604 The expression in Eq. (III-16.25) is applied to both the immediate rewards  $r$  considered in the ML based  
 605 yaw control algorithm presented in this paper and the expression of both matrices  $Q(s,a)$  are obtained and  
 606 presented in Eq. (III-16.26) and Eq. (III-16.27). The discount factor  $\gamma$  is set to 1 in both cases because it is  
 607 considered that all the values in the time horizon are equally important.

$$Q_P(s, a) = \frac{\frac{1}{T} \int_t^{t+T} (P_{\text{control}} - P_{\text{no\_control}}) \cdot dt}{\frac{1}{T} \int_t^{t+T} P_{\text{no\_deviation}} \cdot dt} \cdot 100 \quad [\%] \quad (\text{III-16.26})$$

$$Q_M(s, a) = \int_t^{t+T} \text{RewardM}(t) \cdot dt \quad [N \cdot m] \quad (\text{III-16.27})$$

608 After definition of the states  $s$ , actions  $a$ , immediate rewards  $r$  and the expressions of the matrices  
 609  $Q_P(s,a)$  and  $Q_M(s,a)$ , simulations of the performance of the wind turbine to obtain data for the training  
 610 process of the RL algorithm are carried out. The simulations are carried out with the aeroelastic code FAST  
 611 [63] and the wind turbine model NREL 5MW, presented in the work of Jonkman et al. [14], both designed  
 612 by the National Renewable Energies Laboratory (NREL) in the USA.

613 The objective of the training process of the RL algorithm is to obtain the data related to all possible  
 614 actuation scenarios associated to the yaw control of the wind turbine. Thus, in the design process presented



615 in this chapter, an offline training process of the wind turbine with all the possible considered wind speed  
 616 values and the yaw control actions is proposed. Thus, simulations with StateWindS=3:1:17 [m/s], StateYawA=-90:10:90 [deg], ActionYawK=0.1:0.1:1 [-] and ActionYaw=-90:10:90 [deg] have been carried  
 617 out with the aeroelastic code FAST. The values of the matrices  $Q_P(s,a)$  and  $Q_M(s,a)$  are calculated with  
 618 the data obtained from the simulations, see Eq. (III-16.26) and Eq. (III-16.27).  
 619

620 The fact that the RL training is performed offline indicates that it is independent from the actual operating  
 621 conditions of the wind turbine. Nevertheless, an online training process of the RL algorithm during  
 622 operation of the wind turbine and linked to the actual operating conditions could be possible to keep the  
 623 system learning from real field data and its own experience.

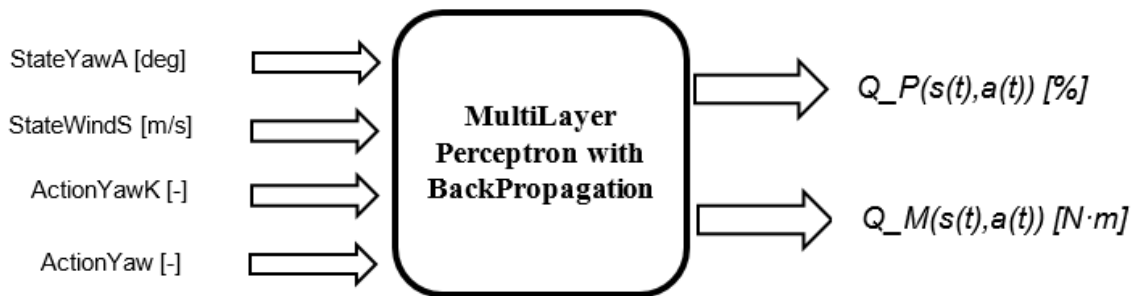
624 **III-16.4.2. Yaw Control MLP-BP**

625 A MLP-BP neural network is designed to store the data of the matrices  $Q_P(s,a)$  and  $Q_M(s,a)$  corresponding to the RL algorithm. The objective of storing these matrices as continuous functions  $Q_P(s(t),a(t))$  and  $Q_M(s(t),a(t))$  is to eliminate the necessity of large amount of data management, which could result problematic in the implementation of the control strategy in the control system of the wind turbine, due to memory issues. Additionally, with the use of an ANN to store the data of the RL algorithm, the replacement policy of the RL algorithm is incorporated, since the ANN learns from the new calculated values. This aspect is of great importance if an online training of the RL algorithm during operation of the wind turbine is implemented. In that case, the ANN continuously learns from new calculated values and the accuracy of the functions  $Q_P(s(t),a(t))$  and  $Q_M(s(t),a(t))$  increase.

634 The selected topology of the ANN designed to store the data of the matrices  $Q_P(s,a)$  and  $Q_M(s,a)$  is a MLP-BP. A MLP-BP is a neural network based on neurons of the type perceptron and with a variable number of hidden layers. The characteristic of the MLP-BP is that the information flow occurs exclusively in the direction from input neurons to output neurons and not in reverse. The BP training process is a supervised training strategy in which the theoretical output of the ANN and the real output of the ANN are compared and the weights of the neurons are adjusted to minimize this error.

640 The designed MLP-BP neural network presents 4 inputs and 2 outputs. A pipeline with the input and outputs of the designed MLP-BP neural network is presented in Figure III-16.8. Internally, the MLP-BP presents a structure with one input layer with 4 neurons, two hidden layers with 75 neurons and 25 neurons respectively and one output layer with 2 neurons.

644



645

646 *Figure III-16.8. Input and outputs of the MLP-BP designed for the ML based yaw control strategy*

647 The learning rate for the training process of the MLP-BP has been set to  $1 \cdot 10^{-50}$ . The training ratio, validation ratio and test ratio have been set to 90 %, 5 % and 5 %, respectively. After the training process, correlation coefficients of 0.9999 and Mean Squared Error (MSE) of  $1.62 \cdot 10^{-6}$  are obtained. The high value of the correlation coefficient and the low value of the MSE are indicators of a correct training process and that the MLP-BP is good enough to be used in the ML based yaw control strategy proposed in this chapter.

652 **III-16.4.3. Yaw Control PSO and PoF**

653 As it was stated in Section III-16.2 of this chapter, the yaw actuation of a wind turbine allows alignment of the rotor of the wind turbine with the direction of the incoming wind and, thus, the power generated by the wind turbine can be maximized in some scenarios. Nevertheless, this power gain is achieved at cost of high mechanical loads in several components of the wind turbine, especially the yaw bearings, which could endanger the safe operation of the wind turbine or reduce its lifetime.

657

658 After carrying out simulations with the aeroelastic code FAST for the training process of the RL algo-  
 659 rithm, the following tendency of the states  $s$  and actions  $a$  corresponding to the RL algorithm has been  
 660 observed:

- 661 - An increased value of the state StateYawA [deg] causes the value of the immediate reward RewardP  
 662 [%] to have greater values. As a result of an increased value of the state StateYawA [deg] the yaw  
 663 actuation is usually more important and the immediate reward RewardM [N·m] is increased.
- 664 - An increased value of the state StateWindS [m/s] makes the value of the immediate reward RewardP  
 665 [%] to be smaller. This fact depends on the wind speed value that determines the operating zone of  
 666 the wind turbine. In some cases, the StateWindS [m/s] is so high that despite the StateYawA [deg]  
 667 the system keeps operating in the rated power zone and no RewardP [%] can be achieved. The  
 668 immediate reward RewardM [N·m] get bigger with greater StateWindS [m/s] values.
- 669 - An increased value of the ActionYawK [-] makes the immediate reward RewardP [%] to be higher,  
 670 since the yaw rotation is performed at a greater rotational speed. The immediate reward RewardM  
 671 [N·m] gets bigger as well.
- 672 - An increased value of the ActionYaw [deg] makes the immediate reward RewardP [%] to be higher,  
 673 since a longer rotation of the wind turbine rotor is allowed. The immediate reward RewardM [N·m]  
 674 gets bigger as well.

675 The objective of the PSO and PoF based optimization algorithm designed in this paper is to obtain a set  
 676 of optimal yaw actions, ActionYawK [-] and ActionYaw [deg], that respond to the compromise necessity  
 677 between RewardP [%] and RewardM [N·m].

678 A pseudocode of the PSO and PoF based optimization algorithm designed for the ML based yaw control  
 679 strategy presented in this chapter is shown in Algorithm III-16.4.  
 680

---

#### PSO and PoF optimization algorithm

---

```

% Initialization
 $\varphi_{1\_max} = \varphi_{1\_max}$ 
 $\varphi_{2\_max} = \varphi_{2\_max}$ 
H = H
P = P           % Population size
n = n           % Number of iterations
a = a_ini(2,P)
% Definition of the states ( $s \in S$ )
s(1)  $\leftarrow$  StateYawA
s(2)  $\leftarrow$  StateWindS
% Start the PSO algorithm
while (iter < n) do
  for 1:1:P
    % Evaluate the current particle
    r = MLP-BP(s,a)
    % Evaluate its introduction to the PoF
    if r(1) < r1_global && r(2) < r2_global
      r_PoF = MLP-BP(s,a_ant)
      PoF = [PoF, r_PoF]
      a_PoF = [a_PoF, a_ant]
    end
  end
  % Generate the new swarm
   $\varphi_1 = \text{random}(\varphi_{1\_max})$ 
   $\varphi_2 = \text{random}(\varphi_{2\_max})$ 
  v  $\leftarrow$  Eq. (III-16.18)
  x  $\leftarrow$  Eq. (III-16.19)
end
end

```

---

681 *Algorithm III-16.4. Pseudocode of the PSO and PoF based optimization algorithm*

682 As it can be observed in **¡Error! No se encuentra el origen de la referencia.**, the output of the PSO  
 683 and PoF optimization algorithm is a set of optimal solutions, known as PoF, that respond to the compromise  
 684 necessity between the power gain and the mechanical loads due to the yaw rotation. To calculate this PoF  
 685 the optimization algorithm makes use of the functions  $Q\_P(s(t),a(t))$  and  $Q\_M(s(t),a(t))$  as the fitness func-  
 686 tions. The states of the system, StateYawA [deg] and StateWindS [m/s], are defined and the fitness value  
 687 of different set of actions, ActionYawK [-] and ActionYaw [deg], is evaluated. The final optimal solutions  
 688 are the solutions in which one of the fitness values cannot be increased without degrading the other one.

689 The implemented PSO and PoF optimization algorithm show correct results in a variety of state scenar-  
 690 ios, StateYawA [deg] and StateWindS [m/s], of the wind turbine:

- 691 - When the wind turbine operates in the partial power zone a more aggressive yaw actuation is trans-  
 692 lated in a higher power gain but at cost of incremented mechanical loads.
- 693 - When the wind turbine operates in the rated power zone and the value of the yaw misalignment is  
 694 high enough to move the operation of the wind turbine out of the rated power zone, a more aggres-  
 695 sive yaw actuation is translated in a higher power gain but at cost of incremented mechanical loads.
- 696 - When the wind turbine operates in the rated power zone and the value of the yaw misalignment is  
 697 not high enough to move the operation of the system out of the rated power zone, a more aggressive  
 698 yaw actuation is translated in zero power gain and incremented mechanical loads, which makes the  
 699 yaw actuation useless.

700 **III-16.4.4. Yaw Control DM**

701 The DM algorithm selects one of the optimal actions proposed as the result of the PSO-PoF optimization  
 702 algorithm. The DM algorithm proposed in this chapter considers the mechanical loads as the limiting factor  
 703 when selecting the yaw actuation and it could be summarized as follows:

- 704 - The solutions that suppose a value of the function  $Q\_M(s(t),a(t))$  higher than a predefined threshold  
 705 are not taken into consideration due to safety issues.
- 706 - From the set of solutions that are taken into consideration, the one with the highest value of the  
 707 function  $Q\_P(s(t),a(t))$  is selected.

708 Other different approaches for the selection of the yaw optimal actuation based on more complex prin-  
 709 ciples could also be evaluated and implemented.

710 **III-16.5. Conclusions**

712 The design procedure of a ML based yaw control algorithm for a HAWT based on AI techniques has  
 713 been presented in this chapter. The proposed yaw control strategy is aimed to improve the performance of  
 714 classical yaw control strategies by means of the use of AI techniques, which emulate the performance of  
 715 natural processes to provide digital systems with intelligence and self-learning capability. The self-learning  
 716 capability is the main characteristic of the ML.

717 The proposed ML based yaw control strategy makes use of three different AI techniques for the devel-  
 718 opment of the control strategy. The RL algorithm maps actions to states and thus allows the development  
 719 of a policy in the wind turbine that selects the best actions in different wind turbine operation scenarios.  
 720 The ANN provides a very important learning capability and allows a continuous learning process in the  
 721 wind turbine, as well as, a simplified data management by storage of large amounts of data as continuous  
 722 functions. Finally, the PSO and PoF based optimization algorithm allows to select the actions that maximize  
 723 the power output of the wind turbine and minimize the mechanical loads generated as a result of the yaw  
 724 rotation.

725 The most important capability of the proposed ML based yaw control strategy is the self-tuning. As a  
 726 result of the self-learning capability of the ML system, there is no need for tuning a closed loop for the yaw  
 727 angle control of the wind turbine. Therefore, the risk associated to a possible inadequate tuning of this  
 728 control loop is erased. In fact, an inadequate control tuning could cause considerable power generation  
 729 losses or high mechanical loads that could endanger the safe operation of the wind turbine.

730 Simulations of the proposed ML based yaw control strategy with the aeroelastic code FAST show prom-  
 731 ising results in comparison to other more simple controllers based on the classical control theory. The most

732 visible improvements are increased generated power values and considerable mechanical load reductions  
 733 in the yaw bearings of the wind turbine for different wind scenarios.

734

735

736 **Funding:** This research was partially funded by Fundation VITAL Fundazioa.

737 **Acknowledgments:** The authors are grateful to the Government of the Basque Country and the University  
 738 of the Basque Country UPV/EHU through the SAIOTEK (S-PE11UN112) and EHU12/26 research pro-  
 739 grams, respectively.

740 **Conflicts of Interest:** The authors declare no conflict of interest.

741

742

## References

- 743 1. Zhao X., Yan Z., Xue Y., Zhang X.: Wind Power Smoothing by Controlling the Inertial Energy of  
 744 Turbines With Optimized Energy Yield, *IEEE Access*, 2017, 5, pp. 23374-23382.
- 745 2. Rosales-Asensio E., Borge-Diez D., Blanes-Peiro J., Perez-Hoyos A., Comenar-Santos A.: Review of  
 746 wind energy technology and associated market and economic conditions in Spain, *Renewable & Sus-  
 747 tainable Energy Reviews*, 2019, 101, pp. 415-427.
- 748 3. WindEurope.: Wind energy in Europe in 2018. Trends and Statistics, 2019.
- 749 4. Nyanteh Y., Schneider N., Netter D., Wei B., Masson P.J.: Optimization of a 10 MW Direct Drive  
 750 HTS Generator for Minimum Levelized Cost of Energy, *IEEE Trans.Appl.Supercond.*, 2015, 25, (3),  
 751 pp. 1-4.
- 752 5. Kim Y.-.: Robust data driven H-infinity control for wind turbine, *Journal of the Franklin Institute*,  
 753 2016, 353, (13), pp. 3104-3117.
- 754 6. Merabet A., Ahmed K.T., Ibrahim H., Beguenane R.: Implementation of Sliding Mode Control Sys-  
 755 tem for Generator and Grid Sides Control of Wind Energy Conversion System, *IEEE Transactions on  
 756 Sustainable Energy*, 2016, 7, (3), pp. 1327-1335.
- 757 7. Watkins C.J.C.H., Dayan P.: Q-learning, *Mach.Learning*, 1992, 8, (3), pp. 279-292.
- 758 8. Erdogmus D., Fontenla-Romero O., Principe J.C., Alonso-Betanzos A., Castillo E.: Linear-least-  
 759 squares initialization of multilayer perceptrons through backpropagation of the desired response, *IEEE  
 760 Trans.Neural Networks*, 2005, 16, (2), pp. 325-337.
- 761 9. Ho S.L., Lo E.W.C., Wong H.C.: A particle swarm optimization-based method for multiobjective  
 762 design optimizations, *IEEE Trans.Magn.*, 2005, 41, (5), pp. 1756-1759.
- 763 10. Zhang D., Han X., Deng C.: Review on the research and practice of deep learning and reinforcement  
 764 learning in smart grids, *CSEE Journal of Power and Energy Systems*, 2018, 4, (3), pp. 362-370.
- 765 11. Yang Z., Merrick K., Jin L., Abbass H.A.: Hierarchical Deep Reinforcement Learning for Continuous  
 766 Action Control, *IEEE Transactions on Neural Networks and Learning Systems*, 2018, 29, (11), pp.  
 767 5174-5184.
- 768 12. Saenz-Aguirre A., Zulueta E., Fernandez-Gamiz U., Lozano J., Lopez-Guede J.M.: Artificial Neural  
 769 Network Based Reinforcement Learning for Wind Turbine Yaw Control, *Energies*, Jan 2019.
- 770 13. Bivona S., Bonanno G., Burlon R., Gurrera D., Leone C.: Stochastic models for wind speed forecast-  
 771 ing, *Stochastic models for wind speed forecasting*, 2010, 52, (2), pp. 1157-1165.
- 772 14. Jonkman J.M., Butterfield S., Musial W., Scott G.: Definition of a 5MW Reference Wind Turbine for  
 773 Offshore System Development, National Renewable Energy Laboratory (NREL), 2009.
- 774 15. J.H. L., L.Y. P., A. W.: Control of Wind Turbines: Past, Present, and Future, *American Control Con-  
 775 ference 2009*, June 2009 St. Louis (USA).
- 776 16. Harris M., Hand M., Wright A.: LIDAR for Turbine Control, NREL Technical Report NREL/TP-500-  
 777 39154., 2005.
- 778 17. M. Y., S. Ö.: Design and Efficiency of 5 kW Wind Turbine Without Gearbox, Controlled by Yaw and  
 779 Pitch Drivers, *Çanakkale Onsekiz Mart Üniversitesi Fen Bilimleri Enstitüsü Dergisi*, 4, (1), pp. 74-  
 780 87.
- 781 18. Ahrens M., Kucera L., Larssonneur R.: Performance of a magnetically suspended flywheel energy  
 782 storage device, *IEEE Transactions on Control System Technology*, 1996, 4, (5), pp. 495-502.

- 783 19. Zheng S., Yang J., Song X., Ma C.: Tracking Compensation Control for Nutation Mode of High-  
784 Speed Rotors With Strong Gyroscopic Effects, *IEEE Trans.Ind.Electron.*, 2018, 65, (5), pp. 4156-  
785 4165.
- 786 20. Shariatpanah H., Fadaeinedjad R., Rashidinejad M.: A New Model for PMSG-Based Wind Turbine  
787 With Yaw Control, *IEEE Trans.Energy Convers.*, 2013, 28, (4), pp. 929-937.
- 788 21. Wang X., Li X., Leung V.C.M.: Artificial Intelligence-Based Techniques for Emerging Heterogene-  
789 ous Network: State of the Arts, Opportunities, and Challenges, *IEEE Access*, 2015, 3, pp. 1379-1391.
- 790 22. Castro P.A.D., Zuben F.J.V.: Learning Ensembles of Neural Networks by Means of a Bayesian Arti-  
791 ficial Immune System, *IEEE Trans.Neural Networks*, 2011, 22, (2), pp. 304-316.
- 792 23. Khanafer R.M., Solana B., Triola J., et al.: Automated Diagnosis for UMTS Networks Using Bayesian  
793 Network Approach, *IEEE Transactions on Vehicular Technology*, 2008, 57, (4), pp. 2451-2461.
- 794 24. Ma H., Simon D., Siarry P., Yang Z., Fei M.: Biogeography-Based Optimization: A 10-Year Review,  
795 *IEEE Transactions on Emerging Topics in Computational Intelligence*, 2017, 1, (5), pp. 391-407.
- 796 25. León-Aldaco S.E.D., Calleja H., Alquicira J.A.: Metaheuristic Optimization Methods Applied to  
797 Power Converters: A Review, *IEEE Transactions on Power Electronics*, 2015, 30, (12), pp. 6791-  
798 6803.
- 799 26. Fadlullah Z.M., Tang F., Mao B., et al.: State-of-the-Art Deep Learning: Evolving Machine Intelli-  
800 gence Toward Tomorrow's Intelligent Network Traffic Control Systems, *IEEE Communications Sur-  
801 veys Tutorials*, 2017, 19, (4), pp. 2432-2455.
- 802 27. Dostál P.: The Use of Optimization Methods in Business and Public Services, Zelinka I., Snášel V.,  
803 Abraham A. (eds) *Handbook of Optimization*. Intelligent Systems Reference Library, 2013, 38,  
804 (Springer, Berlin, Heidelberg).
- 805 28. Jagodnik K.M., Thomas P.S., Bogert A.J.v.d., Branicky M.S., Kirsch R.F.: Training an Actor-Critic  
806 Reinforcement Learning Controller for Arm Movement Using Human-Generated Rewards, *IEEE  
807 Transactions on Neural Systems and Rehabilitation Engineering*, 2017, 25, (10), pp. 1892-1905.
- 808 29. Mongillo G., Shteingart H., Loewenstein Y.: The Misbehavior of Reinforcement Learning, *Proc IEEE*,  
809 2014, 102, (4), pp. 528-541.
- 810 30. Sutton R.S., Barto A.G.: *Reinforcement Learning: An Introduction*, MIT Press, 1998, (Cambridge,  
811 MA, USA).
- 812 31. Kaelbling L.P., Littman M.L., Moore A.W.: Reinforcement learning: A survey, *J. Artif. Intell. Res.*,  
813 1996, 4, (1), pp. 237-285.
- 814 32. Bertsekas D.P.: *Abstract Dynamic Programming*, Belmont, MA, USA:Athena Scientific, 2013.
- 815 33. Bertsekas D.P.: *Dynamic Programming and Optimal Control: Approximate Dynamic Programming*,  
816 Belmont, MA, USA:Athena Scientific, 2012, 2.
- 817 34. Bertsekas D.P.: Value and Policy Iterations in Optimal Control and Adaptive Dynamic Programming,  
818 *IEEE Transactions on Neural Networks and Learning Systems*, 2017, 28, (3), pp. 500-509.
- 819 35. Kao K., Wu I., Yen S., Shan Y.: Incentive Learning in Monte Carlo Tree Search, *IEEE Transactions  
820 on Computational Intelligence and AI in Games*, 2013, 5, (4), pp. 346-352.
- 821 36. Coulom R.: Efficient selectivity and backup operators in Monte-Carlo tree search, *Proc. 5th Int. Conf.  
822 Comput. Games*, 2006, pp. 72-83.
- 823 37. Watkins C.J.C.H.: *Learning from Delayed Rewards*, PhD thesis, King's College, Cambridge, UK,  
824 May 1989.
- 825 38. Adam S., Busoniu L., Babuska R.: Experience Replay for Real-Time Reinforcement Learning Con-  
826 trol, *IEEE Transactions on Systems, Man, and Cybernetics, Part C (Applications and Reviews)*, 2012,  
827 42, (2), pp. 201-212.
- 828 39. Chen S.H., Jakeman A.J., Norton J.P.: Artificial Intelligence techniques: An introduction to their use  
829 for modelling environmental systems, *Mathematics and Computers in Simulation*, 2008, 78, pp. 379-  
830 400.
- 831 40. Yao X.: Evolving artificial neural networks, *Proc. IEEE*, 1999, 87, (9), pp. 1423-1447.
- 832 41. Oong T.H., Isa N.A.M.: Adaptive Evolutionary Artificial Neural Networks for Pattern Classification,  
833 *IEEE Trans.Neural Networks*, 2011, 22, (11), pp. 1823-1836.

- 834 42. Yang X.S.: Optimization and Metaheuristic Algorithms in Engineering, in: *Metaheuristic Algorithms in Water,*  
835 *Geotechnical and Transport Engineering* (Eds. X. S. Yang, A. H. Gandomi, S. Talatahari, A. H. Alavi),  
836 Elsevier, 2013, pp. 1-23.
- 837 43. Jain A.K., Mao J., Mohiuddin K.M.: Artificial neural networks: a tutorial, *Computer*, 1996, 29, (3),  
838 pp. 31-44.
- 839 44. Rounds S.A.: Development of a neural network model for dissolved oxygen in the Tualatin River,  
840 Oregon, *Proceedings of the Second Federal Interagency Hydrologic Modeling Conference*, Las Ve-  
841 gas, NV, 2002.
- 842 45. Wang L., Shen J.: A Systematic Review of Bio-Inspired Service Concretization, *IEEE Transactions*  
843 *on Services Computing*, 2017, 10, (4), pp. 493-505.
- 844 46. Khan B., Singh P.: Selecting a Meta-Heuristic Technique for Smart Micro-Grid Optimization Prob-  
845 lem: A Comprehensive Analysis, *IEEE Access*, 2017, 5, pp. 13951-13977.
- 846 47. Bala A., Ismail I., Ibrahim R., Sait S.M.: Applications of Metaheuristics in Reservoir Computing  
847 Techniques: A Review, *IEEE Access*, 2018, 6, pp. 58012-58029.
- 848 48. Liao T., Socha K., Oca M.A.M.d., Stützle T., Dorigo M.: Ant Colony Optimization for Mixed-Varia-  
849 ble Optimization Problems, *IEEE Transactions on Evolutionary Computation*, 2014, 18, (4), pp. 503-  
850 518.
- 851 49. Xiang Y., Zhou Y., Tang L., Chen Z.: A Decomposition-Based Many-Objective Artificial Bee Colony  
852 Algorithm, *IEEE Transactions on Cybernetics*, 2019, 49, (1), pp. 287-300.
- 853 50. Bandyopadhyay S., Saha S., Maulik U., Deb K.: A Simulated Annealing-Based Multiobjective Opti-  
854 mization Algorithm: AMOSA, *IEEE Transactions on Evolutionary Computation*, 2008, 12, (3), pp.  
855 269-283.
- 856 51. Srinivas M., Patnaik L.M.: Genetic algorithms: A survey, *Computer*, 1994, 27, (6), pp. 17-26.
- 857 52. Anderson-Cook C.M.: *Practical Genetic Algorithms*, Oxfordshire, U.K.: Taylor & Francis, 2005.
- 858 53. Holland J.H.: *Adaptation in Natural and Artificial Systems*, Ann Arbor, MI, USA: Univ. Michigan  
859 Press, 1975.
- 860 54. Kennedy J., Eberhar R.C.: Particle swarm optimization, *Proc. IEEE Int. Conf. Neural Netw.*, Perth,  
861 WA, Australia, Jul 1995, pp. 1942-1948.
- 862 55. Storn R., Price K.: Differential evolution—A simple and efficient heuristic for global optimization  
863 over continuous spaces, *J. Global Optim*, 1997, 11, (4), pp. 341-359.
- 864 56. Ehrgott M., Gandibleux X.: A survey and annotated bibliography of multiobjective combinatorial op-  
865 timization, *OR-Spektrum*, 2000, 22, (4), pp. 425-460.
- 866 57. Durillo J.J., Nebro A.J., Garcia-Nieto J., Alba E.: On the Velocity Update in Multi-Objective Particle  
867 Swarm Optimizers, in Coello Coello C.A., Dhaenens C., Jourdan L. (Eds.): *Advances in Multi-Ob-*  
868 *jective Nature Inspired Computing* (Springer Berlin Heidelberg, Berlin, Heidelberg, 2010, pp. 45-62.
- 869 58. Coello Coello C.A., Dhaenens C., Jourdan L.: Multi-Objective Combinatorial Optimization: Problem-  
870 atic and Context, in Coello Coello C.A., Dhaenens C., Jourdan L. (Eds.): *Advances in Multi-Objective*  
871 *Nature Inspired Computing* (Springer Berlin Heidelberg, Berlin, Heidelberg, 2010, pp. 1-21.
- 872 59. Pareto V.: *Cours D'Economie Politique*, F. Rouge, Lausanne, 1896, I, (II).
- 873 60. Karakasis N., Mesemanolis A., Nalmpantis T., Mademlis C.: Active yaw control in a horizontal axis  
874 wind system without requiring wind direction measurement, *IET Renewable Power Generation*, 2016,  
875 10, (9), pp. 1441-1449.
- 876 61. Song D., Yang J., Fan X., et al.: Maximum power extraction for wind turbines through a novel yaw  
877 control solution using predicted wind directions, *Energy Conversion and Management*, 2018, 157, pp.  
878 587-599.
- 879 62. Bharani R., Jayasankar K.C.: Yaw Control of Wind Turbine Using Fuzzy Logic Controller, *Power*  
880 *Electronics and Renewable Energy Systems*, 2015, 326, pp. 997-1006.
- 881 63. NREL NWTc FAST Version 7. Available online: <https://nwtc.nrel.gov/FAST7/> (accessed on 21 Oct  
882 2018).